Chandra Observations of Hot Gas in Merging Galaxies: Testing Models of Stellar Feedback and Star Formation Regulation

Beverly J. Smith[1], Peter Wagstaff[1], Curtis Struck[2], Roberto Soria[3], Brianne Dunn[1,4], Douglas Swartz[5], Mark L. Giroux[1], Shawn Toner[1]

1) East Tennessee State University, 2) Iowa State University, 3) University of the Chinese Academy of Sciences, 4) Clemson University, 5) NASA Marshall Space Flight Center

ABSTRACT: Feedback from massive stars to the interstellar medium occurs in two stages. In the first stage, stellar winds, radiation, and radiation pressure destroy molecular clouds around young stars, and heat and stir the gas. Then supernovae occur. The effectiveness of the first phase in destroying molecular clouds affects how easily the hot gas produced by supernovae escapes from the region, and how much X-ray emission is produced. To test these models, we measured the hot gas content in 49 nearby merging galaxies, and compared with the SFR and the density of young stars.

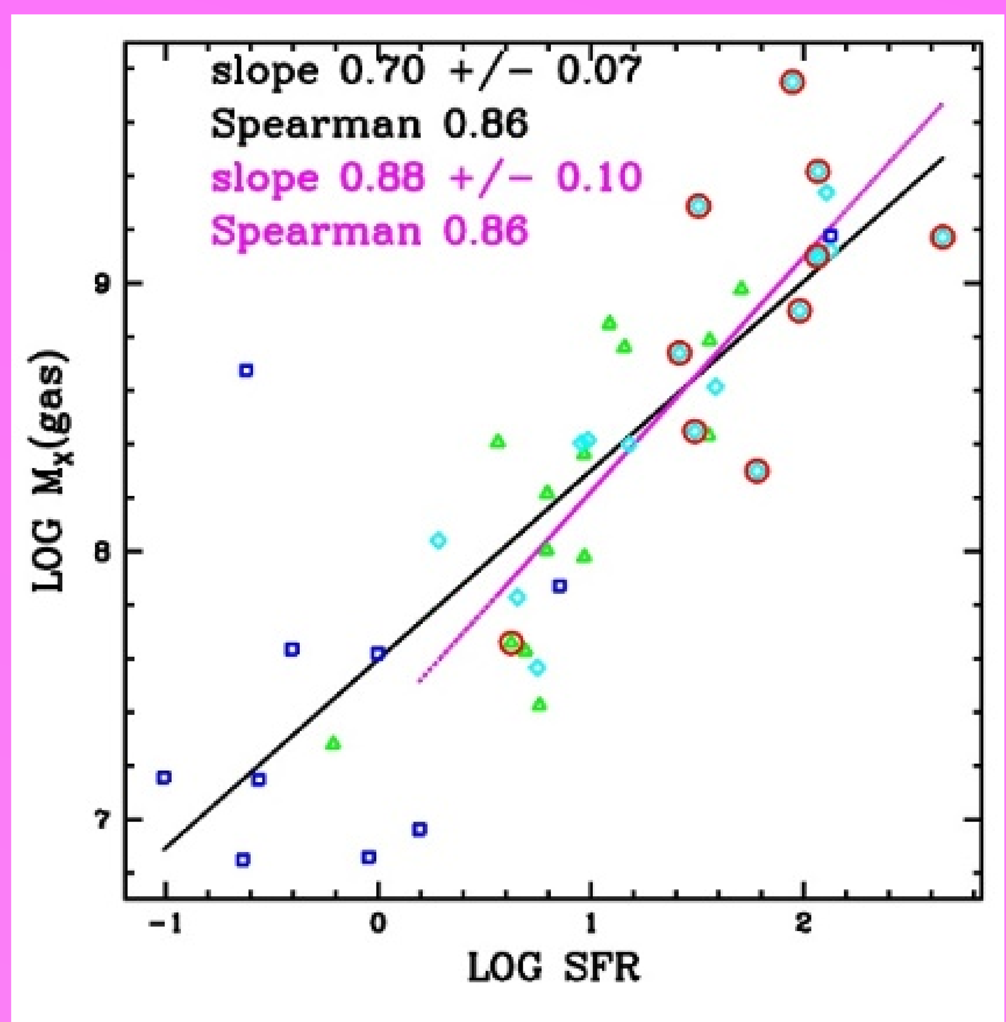

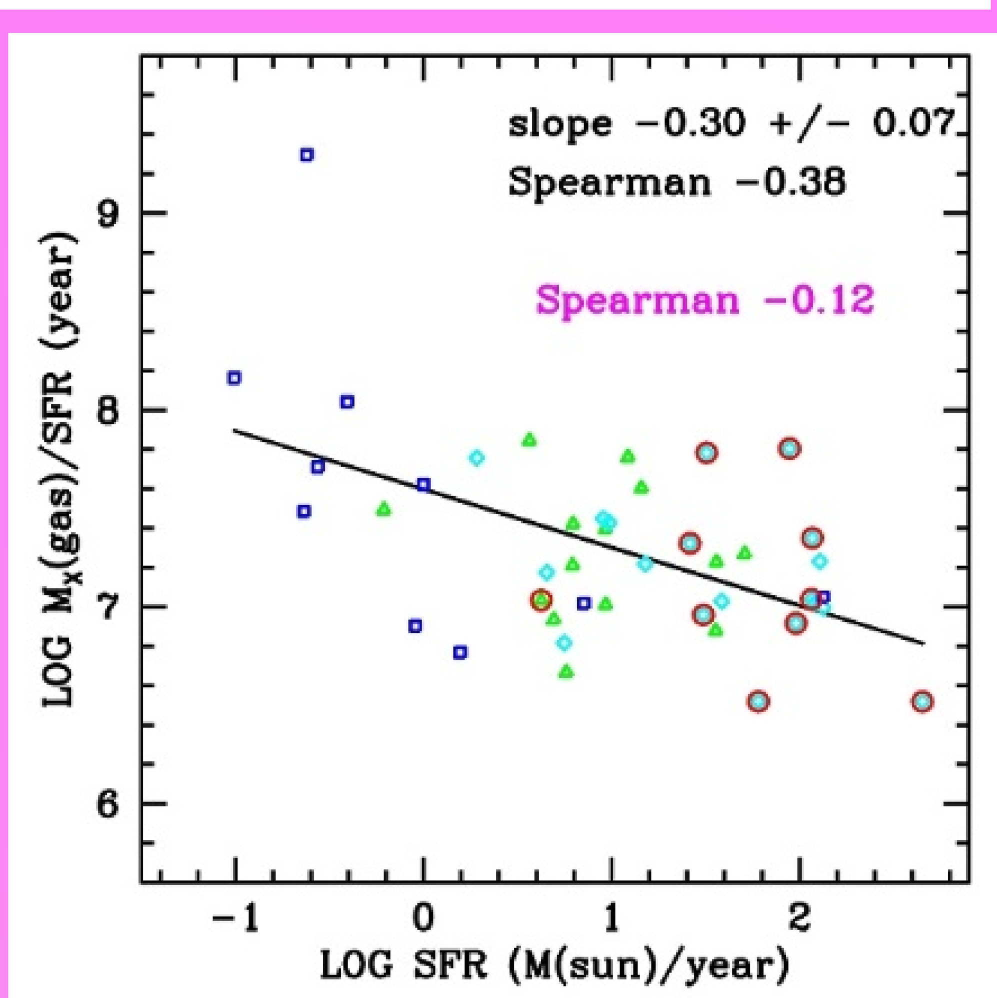

Blue squares: Late-stage mergers

Green triangles: pre-mergers

Cyan diamonds: mid-mergers

AGN (red circles) do not stand out in plots.

The low SFR galaxy with the highest M_X(gas)/SFR is the post-starburst post-merger NGC 1700

In the plots, the magenta lines and best-fit values are for SFR > 1 solar mass/year.

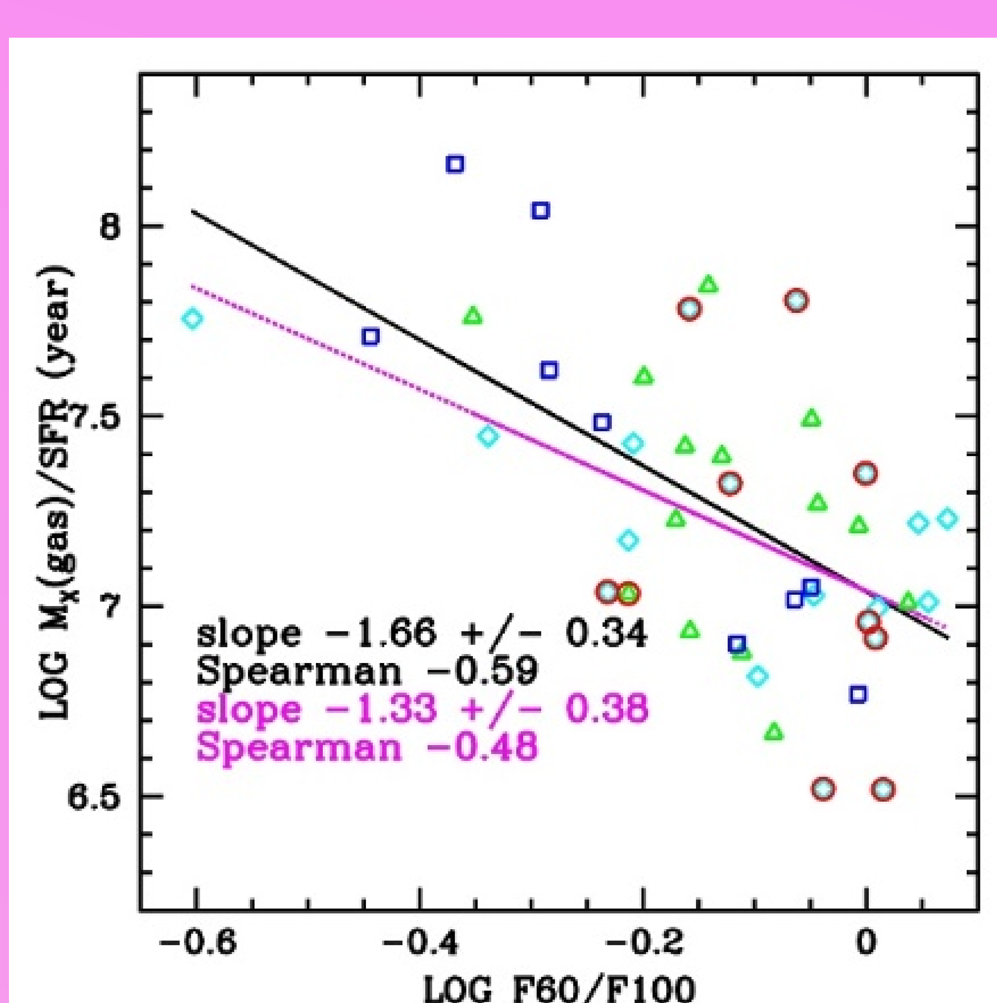

Left (top): Mass of hot gas correlates with SFR. There is possible excess hot gas at low SFRs. Left (middle): M_x(gas)/SFR constant with SFR, except higher M_X(gas)/SFR at low SFR. Right: No trend with merger stage is apparent, except a few post-mergers (stage 7) show excesses. These are known post-starburst systems.

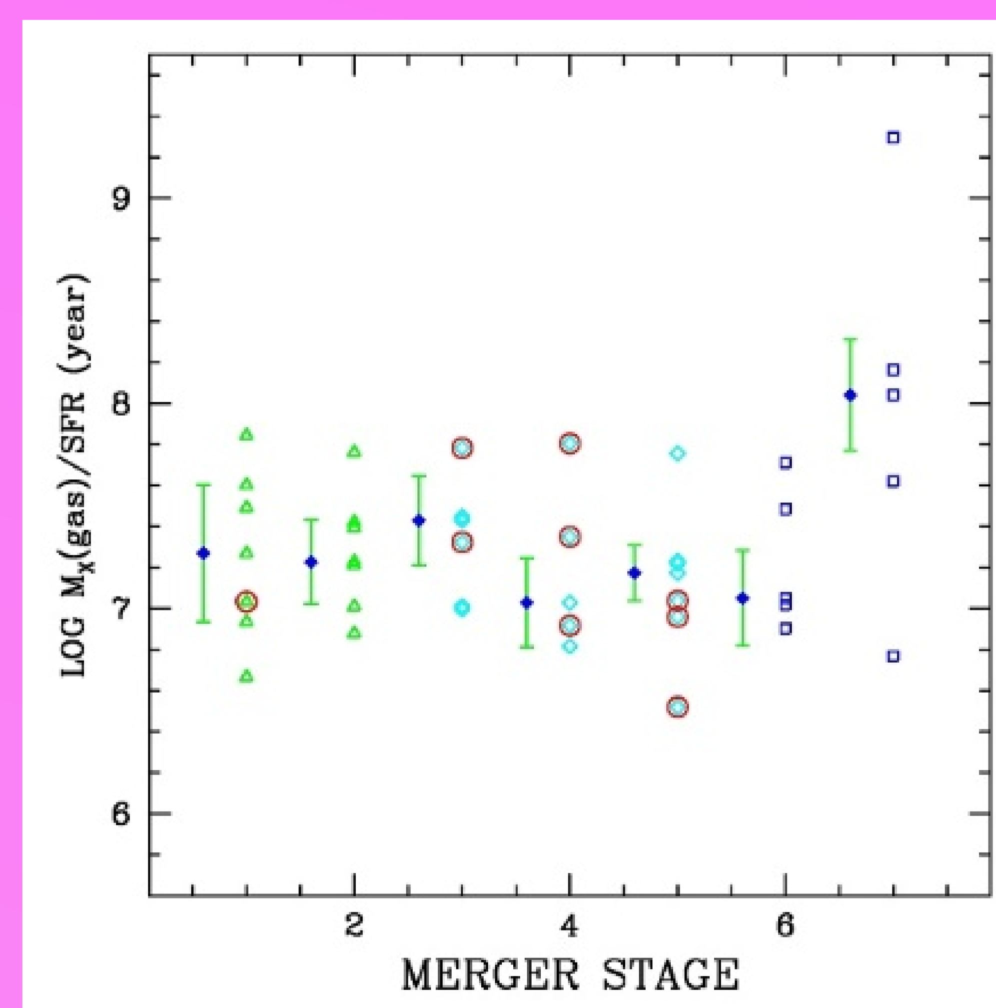

Blue filled diamonds (above): median value per merger stage

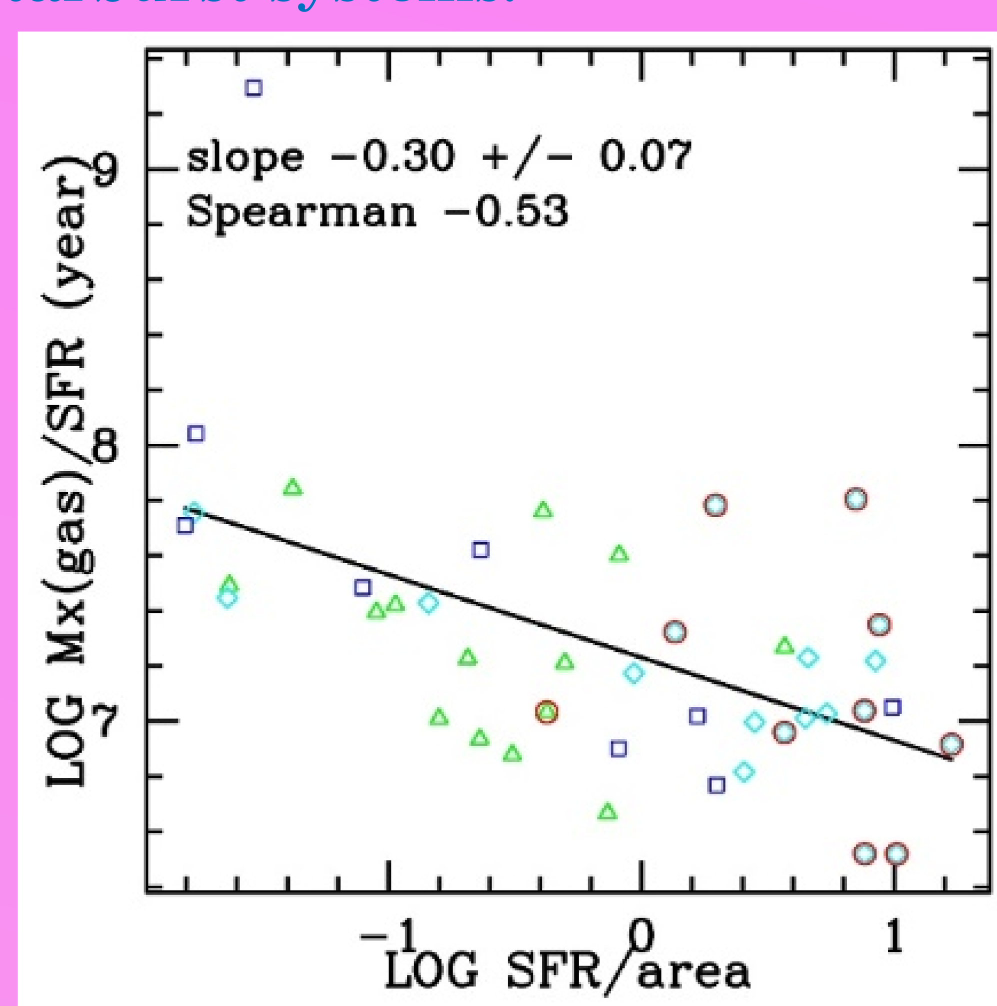

Hot gas volume also correlates with SFR, as does M_X(gas)/M(cold gas) (plots not shown).

M_X(gas)/SFR is anti-correlated with IRAS F_{60}/F_{100} ratio (left) and with SFR/area (above). F_{60}/F_{100} is a measure of average dust temperature, and so a measure of the spatial density of young stars. Area measured using the Spitzer 8 micron effective radius. More young stars per volume means more early stellar feedback, thus supernovae occur in lower density material and hot gas escapes more readily. This produces less X-ray emission per SFR. Confined hot gas produces more X-rays than freely-flowing gas.

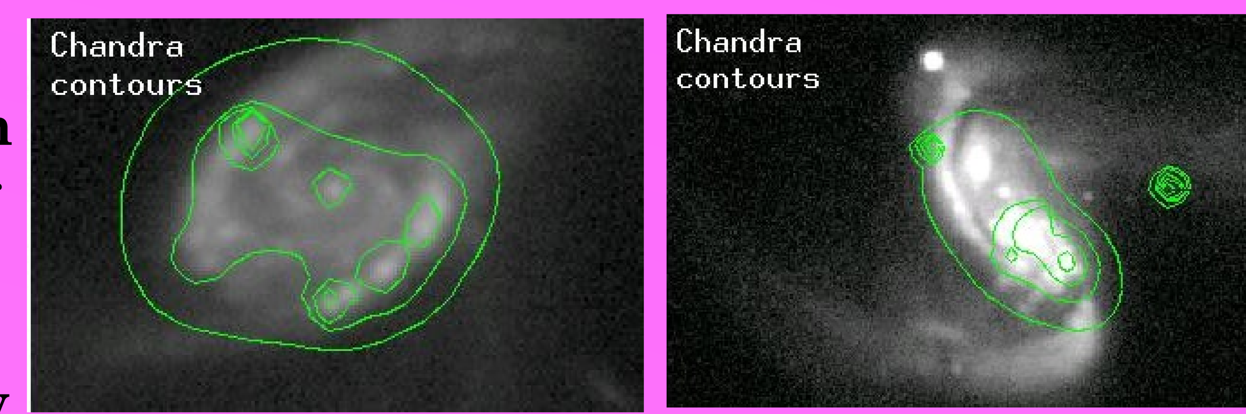

SDSS g image of Arp 240N (left) and Arp 240S (right), with Chandra X-ray contours (Smith et al. 2014)

SAMPLE: 49 nearby major mergers, including pre-merger pairs, mid-merger systems, and post-merger remnants. Selected based on availability of Chandra archive data.

ANALYSIS:

1) Identified and removed bright point sources Statistics on point sources analyzed separately (Smith et al. 2012).

2) Extracted X-ray spectrum of diffuse light.

3) Fit two components, thermal and power law. The thermal component (mostly lower energy) assumed to be from hot gas; power law component (mostly higher energy) assumed from faint unresolved point sources.

4) Used radial profiles assuming an elliptical distribution to measure the spatial extent of the diffuse soft X-ray light (0.3 – 1.0 keV) to a consistent X-ray surface brightness of 3 x 10^{-9} photons s^{-1} cm^{-2} $arcsec^{-2}$. This contains ~90% total light.

5) Calculated volume of hot gas assuming line of sight extent equal to average of the other two dimensions.

6) Used volume and the X-ray luminosity to calculate average density of the hot gas and the mass of hot gas.

7) SFR from UV+IR as in Hao et al. (2011)

CONCLUSIONS: Star formation is powering the hot gas in these galaxies. AGN feedback and shock heating from the direct impact of two gaseous disks (as in the Taffy galaxies; Appleton et al. 2015) are not important contributors to the observed hot gas in our sample. Low SFR post-starburst systems show excess hot gas. Higher spatial densities of young stars produce more hot gas per SFR consistent with theoretical expectations.

More details of the analysis is provided in Smith et al. (2018, 2019).

References:

Appleton et al. (2015), ApJ, 812, 118

Hao et al. (2011), ApJ, 741, 124;

Smith et al. (2012), AJ, 143, 144;

Smith et al. (2014), AJ, 147, 60;

Smith et al. (2018), AJ, 155, 81;

Smith et al. (2019), AJ, 158, 169.

ACKNOWLEDGMENTS: NASA Chandra Telescope Grant AR-17009X